PHYSICAL REVIEW B VOLUME 1, NUMBER 10 15 MAY 1970

Lindemann Law and Lattice Dynamics

J. N. SHAPIRO
Department of Physics, University of California, Los Angeles, California 90024

(Received 6 October 1969)

Using lattice dynamics, the Lindemann law of melting has been tested for five body-centered and six face-centered metallic elements. The law is obeyed by all five of the bcc alkali metals; the average Lindemann parameter is 0.113. Four of the six fcc metals, Al, Cu, Ag, and Au, also obey the law with an average value for the Lindemann parameter of 0.071. Explanations are proposed why the agreement of Ni and Pb with the fcc value is not as good. The improvements are obtained by the use of spectral moments and data, where available, on physical properties at high temperature. The slopes of the melting curves have been calculated and are found to be consistently lower than the values experimentally determined, probably because of the unavailability of data on properties at high temperature.

INTRODUCTION

It was hypothesized by Lindemann[1] that the melting temperature of a material is attained when the root-mean-square amplitude of atomic vibration becomes a certain fraction δ of the nearest-neighbor distance. It was proposed that this fraction, the so-called Lindemann parameter, might be the same for all materials, even at high pressures. Lindemann confined his treatment to polycrystals in the Einstein approximation; comparisons were made mainly using room-temperature data.

Gilvarry[2] attempted to update the Lindemann law and used data taken at the melting point. More recently, Singh and Sharma[3] applied the methods of lattice dynamics to this problem. These authors used a numerical method to sample roots of the secular equation but employed room-temperature elastic data.

In this paper, we shall treat the frequency spectrum analytically by means of the moment trace method.[4] Nearest- and next-nearest-neighbor central interactions are treated and relations due to Fuchs[5] are employed to determine the force constants. Elastic constants and lattice constants extrapolated to the melting point will be used. In addition, the statistical excitation of the modes will be taken into account.

LINDEMANN LAW FROM A LATTICE DYNAMICAL STANDPOINT

The mean-square amplitude of oscillation of a monatomic crystal lattice is given by Blackman[6] as

$$\langle u^2\rangle = \frac{1}{3mN}\sum_{\mathbf{k},j}\frac{E_{\mathbf{k}j}}{\omega_j^2(\mathbf{k})} = \frac{1}{3mN}\sum\frac{1}{\omega_j^2(\mathbf{k})}\frac{\hbar\omega_j(\mathbf{k})}{(e^{\hbar\omega_j(\mathbf{k})/K_BT}-1)}, \quad (1)$$

where m is the atomic mass, N is the number of atoms, and $E_{\mathbf{k},j}$ and $\omega_j(\mathbf{k})$ are the average energy and angular frequency of a phonon of wave number $\mathbf{k}$ and polarization j. The zero-point energy is here neglected.

Inserting the Lindemann statement as $\langle u^2\rangle=\delta^2d^2$ with d, the nearest-neighbor spacing, and expressing the sums as integrals, Eq. (1) becomes

$$\delta^2d^2=\frac{1}{3mN}\int_0^{\omega_L}\frac{g(\omega)}{\omega^2}\frac{\hbar\omega}{(e^{\hbar\omega/K_BT_M}-1)}d\omega. \quad (2)$$

Here $g(\omega)$ is the usual frequency distribution function and ω_L is the maximum lattice frequency. Also, the temperature is now subscripted by an M to indicate that the Lindemann relation is expected to hold at the melting point.

SECULAR DETERMINANTS AND FORCE CONSTANTS

The secular determinants for body- and face-centered lattices with nearest- and next-nearest-neighbor central forces are given by deLaunay.[7] By applying the relations of Fuchs[5] to the long-wavelength expansion of the determinants, the force constants α_1 and α_2 for first and second neighbors, respectively, can be related to the elastic constants. deLaunay finds

$$\alpha_1=\tfrac{3}{2}ac_{44}, \quad \alpha_2=\tfrac{1}{2}a(c_{11}-c_{12})\,; \qquad \text{bcc} \quad (3)$$

$$\alpha_1=ac_{44}, \quad \alpha_2=\tfrac{1}{4}a(c_{11}-c_{12}-c_{44})\,, \quad \text{fcc} \quad (4)$$

with a the lattice parameter.

For most metals, the potential decays rather rapidly beyond the first few neighbors. The rate of decay can be tested by examining the ratio α_2/α_1. When $\alpha_2/\alpha_1\ll1$, it is likely that the effects of atoms more distant than the second neighbors can be safely neglected. Table I gives the ratio α_2/α_1 for 12 bcc and 10 fcc elements using Eqs. (3) and (4). If α_2/α_1 is not small, the addition of more neighbors becomes necessary and the values of α_1

---

[1] F. A. Lindemann, Z. Physik **11**, 609 (1910).

[2] J. J. Gilvarry, Phys. Rev. **102**, 308 (1956); **103**, 1700 (1956); **104**, 909 (1956).

[3] A. K. Singh and P. K. Sharma, Can. J. Phys. **46**, 1677 (1968).

[4] E. W. Montroll, J. Chem. Phys. **10**, 218 (1942); **11**, 481 (1943).

[5] K. Fuchs, Proc. Roy. Soc. (London) **A153**, 622 (1935); **A157**, 444 (1936).

[6] M. Blackman, Proc. Cambridge Phil. Soc. **33**, 380 (1937).

[7] J. deLaunay, Solid State Phys. **2**, 219 (1956).

TABLE I. Elastic constants and the ratio α_2/α_1 for some cubic elements (at $T=300°\text{K}$, unless otherwise noted[a]).

Element	c_{11}	c_{12}	c_{44}	$\frac{1}{3}\frac{c_{11}-c_{12}}{c_{44}}=\frac{\alpha_2}{\alpha_1}$
	(10^{12} dyn/cm^2)			
bcc				
Cr	3.50	0.68	1.01	0.93
Cs[b] (78°K)	0.0247	0.0206	0.0148	0.092
Fe	2.30	1.35	1.14	0.28
K	0.0457	0.0374	0.0263	0.11
Li	0.134	0.112	0.096	0.076
Mo	4.41	1.72	1.22	0.73
Na	0.0739	0.0622	0.0419	0.093
Nb	2.46	1.34	0.287	1.3
Rb[c] (78°K)	0.0325	0.0273	0.0198	0.088
Ta	2.61	1.57	0.818	0.42
V	2.28	1.19	0.426	0.85
W	5.15	2.04	1.56	0.66
fcc				$\frac{1}{4}\left(\frac{c_{11}-c_{12}-c_{44}}{c_{44}}\right)=\frac{\alpha_2}{\alpha_1}$
Ag	1.22	0.92	0.446	−0.082
Al	1.09	0.63	0.280	+0.16
Au	1.89	1.59	0.426	−0.074
Cu	1.69	1.22	0.754	−0.094
Ni	2.48	1.53	1.16	−0.045
Pb	0.481	0.408	0.146	−0.13
Pd	2.27	1.76	0.717	−0.072
Th	0.753	0.489	0.478	−0.11
Ir[d] (0°K)	5.80	2.42	2.56	+0.080
Pt[e]	3.467	2.507	0.765	+0.064

[a] Unless otherwise stated, all data are from Hearmon (see Ref. 10).
[b] F. J. Kollarits and J. Trivisonno, J. Phys. Chem. Solids **29**, 2133 (1968).
[c] See Ref. 18.
[d] See Ref. 14.
[e] See Ref. 12.

and α_2 will, in general, be altered. In fact, when more than two sets of neighbors are included a unique determination of the force constants from the macroscopic first order elastic constants is no longer possible.

For fcc lattices the last column in Table I is generally smaller in magnitude than for the bcc cases. The ratios of second to first neighbor distances are $2/\sqrt{3}=1.155$ for bcc and $\sqrt{2}=1.414$ for fcc. Thus, it seems reasonable that a bcc lattice, in which the second neighbors are somewhat closer will have larger force constant ratios on the average than fcc structures.

Both α_1 and α_2 are positive for the bcc elements in Table I. For the fcc metals, on the other hand, all have a positive α_1, and, with the exception of Al, Ir, and Pt, a negative α_2. Thus it appears that for the fcc metals except Al, Ir, and Pt, the potential well is sufficiently narrow for the second neighbors to be beyond the inflection point of the interatomic potential.

A qualitative criterion must be defined to determine which of the metals of Table I are probably best described by a two-constant model. We consider all metals for which α_2/α_1 is approximately less than $\frac{1}{4}$. Hence bcc metals Cr, Mo, Nb, Ta, V, and W are not considered; all fcc entries meet this criterion. Iron is a borderline case which would be retained were it not for the fact that the α phase for which elastic data are available does not melt[8] at zero pressure.

MATRIX MOMENT METHOD

The spectrum $g(\omega)$ is calculated by the moment-trace method of Montroll.[4] Since the secular equation is a cubic in ω^2 and since the coefficients involve trigonometric functions it is possible to sum the N equations in closed form to obtain, in principle, all even moments $\langle\omega^{2n}\rangle$ of the distribution. The spectrum is expanded in Legendre polynomials of even order and the coefficients of expansion can be expressed in terms of the even moments.

The calculation of $g(\omega)$ for simple and body-centered lattices has been performed by Montroll,[4] and Montroll and Peaslee,[9] respectively. Their procedure is extended in the Appendix to include face-centered lattices. Let $g(x)dx$ represent the number of frequencies between x and $x+dx$, $0\leq x\leq 1$. We find

$$g_b(x_b)=3N\sum_{s=0}^{7}x_b^{2s}\sum_{m=0}^{7}c_{sm}{}^{b}\tau^m\,,\tag{5}$$

$$g_f(x_f)=3N\sum_{s=0}^{6}x_f^{2s}\sum_{m=0}^{6}c_{sm}{}^{f}\gamma^m\,,\tag{6}$$

with

$$\begin{aligned}&\text{bcc}\\ \tau&=(1+\tfrac{3}{4}\alpha_2/\alpha_1)^{-1}\\ &=4c_{44}/(c_{11}-c_{12}+4c_{44})\,,\\ \omega_L{}^b&=[4(4\alpha_1+3\alpha_2)/3m]^{1/2}\\ &=[2a(c_{11}-c_{12}+4c_{44})/m]^{1/2}\,,\\ x_b&=\omega/\omega_L{}^b\,,\\ &\text{fcc}\\ \gamma&=1+\alpha_2/2\alpha_1\\ &=1+(c_{11}-c_{12}-c_{44})/8c_{44}\,,\\ \omega_L{}^f&=(8\alpha_1/m)^{1/2}\\ &=(8c_{44}a/m)^{1/2}\,,\\ x_f&=\omega/\omega_L{}^f\,,\end{aligned}\tag{7}$$

where the 64 coefficients $c_{sm}{}^b$ are given by Montroll and Peaslee[9] and the 49 coefficients $c_{sm}{}^f$ are found in Table VIII. The expansion for fcc lattices performed in the Appendix was carried through the twelfth moment. Montroll and Peaslee use one more moment; hence the upper limits in the sums are different in the fcc and bcc cases.

MOMENT METHOD AND LINDEMANN LAW

Expressions (5) and (6) considered as functions of x each contain a constant term, whereas it is well known[7]

---

[8] K. F. Sterrett, W. Klement, Jr., and G. C. Kennedy, J. Geophys. Res. **70**, 1979 (1965).

[9] E. W. Montroll and D. C. Peaslee, J. Chem. Phys. **12**, 98 (1944).

that

$$g(x) \underset{x\to 0}{=} O(x^2).$$

This nonphysical term, a necessary consequence of the approximate moment scheme, causes the integral ofEq. (2) to diverge. This difficulty can most easily be surmounted by simply neglecting the small constant term in (5) and (6); alternatively one can also express the spectrum for small x by the first term in a Taylor's series about the origin. We have chosen the first approach.

We substitute Eqs. (5) and (6) into Eq. (2). For the face-centered lattice $d=a/\sqrt{2}$ and Eq. (2) becomes

$$\delta_f{}^2a^2=\frac{2}{m}\sum_{m=0}^{6}\gamma^m\sum_{s=1}^{6}c_{sm}{}^f\int_0^{\omega_L}\frac{x^{2s}}{\omega^2}\frac{\hbar\omega}{(e^{\hbar\omega/K_BT_M}-1)}\frac{d\omega}{\omega_L{}^f}. \tag{8}$$

Setting

$$u=\hbar\omega/K_BT_M\,,\quad u_L{}^f=\hbar\omega_L{}^f/K_BT_M$$

and using Eq. (7),

$$\delta_f{}^2=K_BT_My_f/4c_{44}a^3\,, \tag{9}$$

where

$$y_f=\sum_{m=0}^{6}\gamma^m\sum_{s=1}^{6}c_{sm}{}^fG(u_L{}^f{}_s)\,,$$

and

$$G(u,s)=\int_0^u\left(\frac{z}{u}\right)^{2s-1}\frac{dz}{(e^z-1)}.$$

By expanding $z/(e^z-1)$ in a power series in z,

$$\frac{z}{e^z-1}=1-\tfrac{1}{2}z+\frac{B_1z^2}{z!}-\frac{B_2z^4}{4!}+\cdots\,, \tag{10}$$

we find

$$G(u,s)\cong\frac{1}{2s-1}-\frac{u}{4s}+\frac{u^2}{12(2s+1)}-\frac{u^4}{720(2s+3)}+\frac{u_6}{30\,240(2s+5)}-\frac{u^8}{1\,209\,600(2s+7)}\,, \tag{11}$$

which holds to within one part in 10^6 for all cases treated in this paper.

For the body-centered structure the analogous algebra gives

$$\delta_b{}^2=2K_BT_My_b/3(c_{11}-c_{12}+4c_{44})a^3\,, \tag{12}$$

where

$$y_b=\sum_{m=0}^{7}\tau^m\sum_{s=1}^{7}c_{sm}{}^bG(u_L,{}^b\ s).$$

The coefficient δ has been assigned subscripts to allow for the possibility that it is dependent upon structure.

ELASTIC CONSTANTS AND LATTICE PARAMETERS AT FUSION

The metals listed in Table I were selected because measurements of the lattice constants are available as a function of temperature. In some cases it has been found[10] that at temperatures above about 50°K the constants decrease linearly over a range of several hundred degrees.[11] The elastic constants of Pt[12] and Pd[13] do not vary linearly with temperature within the limits of experimental error. Therefore we do not attempt to predict values of the elastic constants for Pt and Pd at the melting point with any degree of certainty. Only the variation of c_{44} with temperature is available for Ir[14]; Ir is also excluded in this calculation.

Th is unusual; although c_{11} and c_{44} decrease with temperature as expected, c_{12} increases linearly, at least throughout the range from 77 to 400°K.[15] We do not know if the anomalous behavior persists at higher temperatures. In any case thorium undergoes a polymorphic transition betow the zero-pressure melting point. Pt, Pd, Ir, and Th have been excluded from further consideration.

Table II lists the pertinent parameters for the remaining eleven metals. The coefficient of thermal expansion, α, at elevated temperatures is difficult to obtain experimentally but, for our purposes, happens not to be crucial. Cs and Rb have zero-pressure melting points sufficiently close to room temperature that corrections to the density at 300°K are unnecessary. The density of Li at melting was determined by a linear extrapolation from the values at 78°K[16] and 300°K.[17]

Recent measurements of the elastic constants of Cu, Ag, and Au have been made over a range of temperatures up to about 80% of melting.[11] These are considered as separate cases so that we may investigate the effects of small changes in the values of the elastic constants on the Lindemann parameter.

DISCUSSION AND RESULTS

Tables III and IV list the values of the Lindemann parameter and other pertinent parameters at the melting point for the five body-centered alkali metals and six face-centered metals, respectively. The value of δ cluster about 0.113 for the bcc lattices and 0.071 for the

---

[10] R. F. S. Hearmon, in *Zahlenwerte and Funktionen, New Series, Group III*, edited by H. Landolt and R. Bornstein (Springer-Verlag, Berlin, 1966), p. 1.

[11] Y. A. Chang and L. Himmel, J. Appl. Phys. **37**, 3567 (1966).

[12] R. E. MacFarlane, J. A. Rayne, and C. K. Jones, Phys. Letters **18**, 91 (1965).

[13] J. A. Rayne, Phys. Rev. **118**, 1545 (1960).

[14] R. E. MacFarlane, J. A. Rayne, and C. K. Jones, Phys. Letters **20**, 234 (1966).

[15] P. E. Armstrong, O. N. Carlson, and J. F. Smith, J. Appl. Phys. **30**, 36 (1959).

[16] H. C. Nash and C. S. Smith, ONR Research Report No. 140628, Case Institute of Technology, Cleveland, Ohio, 1958 (unpublished).

[17] *Handbook of Chemistry and Physics* (Chemical Rubber Publishing Co., Cleveland, Ohio, 1959), 40th ed.

TABLE II. Elastic constants at fusion and T_M, ρ, α, and M for eleven cubic elements.

Element	T_M (°K)	$c_{11}(T_M)$	$c_{12}(T_M)$ (10^{12} dyn/cm^2)	$c_{44}(T_M)$	$\rho(300)$ (g/cm^3)	α (10^{-4}°K^{-1})	M
fcc							
Li	459	0.1266[a]	0.1064[a]	0.0739[a]	0.534[b]	...	6.94
Na	370.7	0.0709[c]	0.0599[c]	0.0370[c]	0.971[d]	2.75[e]	23.00
K	335.2	0.0363[f]	0.0310[f]	0.0172[f]	0.851[f]	2.5[e]	39.10
Rb	311.7	0.0269[g]	0.0230[g]	0.0130[g]	1.53[b]	...	85.48
Cs	301.7	0.0218[h]	0.0186[h]	0.0107[h]	1.873[b]	...	132.91
bcc							
Al	932.7	0.683[i]	0.403[i]	0.188[i]	2.699[d]	0.99[e]	26.97
I		1.315[i]	1.053[i]	0.4833[i]			
Cu	1356				8.937[j]	0.70[e]	63.54
II		1.269[j]	1.018[j]	0.470[j]			
I		0.958[i]	0.791[i]	0.279[i]			
Ag	1233.8				10.50[j]	0.81[e]	107.88
II		0.916[j]	0.764[j]	0.287[j]			
I		1.538[i]	1.343[i]	0.294[i]			
Au	1336				19.30[j]	0.58[e]	197.00
II		1.572[j]	1.380[j]	0.281[j]			
Pb	600.4	0.419[i]	0.374[i]	0.100[i]	11.34[b]	1.2[e]	207.21
Ni	1728	1.52[i]	1.42[i]	0.66[i]	8.90[b]	0.57[c]	58.69

[a] T. Slotwinski and J. Trivisonno, J. Phys. Chem. Solids **30**, 1276 (1969).
[b] See Ref. 17.
[c] M. E. Diederich and J. Trivisonno, J. Phys. Chem. Solids **27**, 637 (1966).
[d] O. L. Anderson, in *Physical Acoustics* (Academic Press Inc., New York, 1965), Vol. III, Part B.
[e] O. Kubaschewski, Trans. Faraday Soc. **45**, 931 (1949).
[f] W. R. Marquardt and J. Trivisonno, J. Phys. Chem. Solids **26**, 273 (1965).
[g] See Ref. 18.
[h] F. J. Kollarits and J. Trivisonno, J. Phys. Chem. Solids **29**, 2133 (1968).
[i] See Ref. 10.
[j] See Ref. 11.

fcc lattices. These can be compared with Gilvarry's values of 0.13 and 0.11, respectively obtained by an analysis based on the Debye-Waller theory, strictly applicable only to polycrystals. Only one bcc element considered by Gilvarry appears in Table III with the result $\delta_{Na}=0.094$. Those fcc elements listed both in Table IV and in Gilvarry's analysis have a mean value of δ_f of 0.083 in the latter case. These values are in only slightly better agreement with ours. Significantly, the values of δ in Tables III and IV have a smaller scatter.

The factor

$$\hbar\omega/e^{\hbar\omega/K_BT_M}-1$$

has been neglected previously, both by Gilvarry and by Singh and Sharma on the assumption that, at melting $K_BT_M\gg\hbar\omega$, for all modes and hence $u_L\ll 1$. This is incorrect for a number of materials listed here. If we had assumed that $u_L\cong 0$, in the worst case, namely, that of Li, we would have obtained a value $\delta=0.124$ instead of 0.116. Inclusion of this feature would have improved the results of Singh and Sharma somewhat. Even so, Singh and Sharma neglected the significant decreases in the elastic constants with temperature.

TABLE III. Results for bcc elements.

Element	δ_b	$u_L{}^b$	τ	α_2/α_1	$\rho(T_M)$ (g/cm^3)	$a(T_M)$ Å	y
Lithium	0.116	0.731	0.936	0.091	0.526	3.525	4.40
Sodium	0.111	0.390	0.931	0.099	0.952	4.313	4.60
Potassium	0.112	0.252	0.928	0.103	0.844	5.359	4.64
Rubidium	0.115	0.164	0.930	0.100	1.530	5.704	4.75
Cesium	0.111	0.128	0.930	0.100	1.873	6.177	4.83

If 0.113 is chosen as an average value for δ_b in Table III, the deviation is less than 3% whereas the accuracy of the raw data (before extrapolation) is typically of the same order.[18] The extrapolations are made over a range in which the elastic constants decrease by as much as 20 or 30%. The results are then certainly within the experimental error in this case.

The mean of the fcc values of the Lindemann parameter is 0.071 and a slightly larger scatter arises compared with the case of the bcc metals. The scatter is probably greater than the limits of error of the initial data. However, most of the available derivatives of elastic constants with temperature are evaluated at 300°K [10] and the extrapolations to the melting tempera-

TABLE IV. Results for fcc elements.

Element		δ_f	$u_L{}^f$	γ	α_2/α_1	$\rho(T_M)$ (g/cm^3)	$a(T_M)$ Å	y
Aluminum		0.072	0.305	1.061	+0.122	2.535	4.134	2.13
Copper	I	0.068	0.208	0.943	−0.110	8.300	3.705	2.43
	II	0.069	0.205	0.942	−0.120			2.43
Silver	I	0.071	0.141	0.950	−0.100	9.735	4.191	2.43
	II	0.071	0.143	0.941	−0.120			2.58
Gold	I	0.073	0.099	0.958	−0.084	18.170	4.160	2.45
	II	0.075	0.097	0.960	−0.070			2.47
Lead		0.065	0.137	0.931	−0.140	10.940	5.011	2.57
Nickel		0.077	0.196	0.894	−0.210	8.200	3.622	3.11

---

[18] E. J. Gutman and J. Trivisonno, J. Phys. Chem. Solids **28**, 805 (1967).

tures, which are much greater than those of the alkali metals, are much less reliable. However, measurements are available for Cu, Ag, and Au to 800°K [11]; these are listed as II in Table IV. Al gives a result consistent with that of these three metals, which are themselves internally consistent. We conclude that the values of δ for bcc and fcc metals are significantly different; Lindemann's law holds for each structure separately.

This conclusion is in direct contrast with the results of Cartz.[19] Cartz combined the Debye theory with the single-frequency Einstein assumption and obtained the same average Lindemann parameter for four selected body-centered elements and several face-centered elements.

The large value of δ for nickel may be attributed mainly to the relatively large value for y_f. This apparently does not arise due to an abnormal value for u_L^f. However γ is smaller for Ni than for the other fcc metals and probably related to the fact that, at melting, α_2/α_1 is -0.21 and is only -0.045 at room temperature. The change in α_2/α_1 seems large when compared with the other materials. This apparent anomaly may arise from the dependence of the elastic constants on temperature.[10,20] c_{11} exhibits a slight kink at the Curie temperature while the plot of c_{12} against T is highly nonlinear throughout the entire range from 4.2 to 750°K. Part of this complication may arise from magnetic contributions to the constants below the Curie point.[20] Extrapolation of the data from the Curie point to melting may be questionable. This applies most strongly to c_{12}, and somewhat less so to c_{11}. c_{44} appears to be linear above 300°K. If the value $y=2.50$ were used for nickel typical of the other fcc metals then $\delta_f=0.069$ in substantial agreement with the first four entries.

The case of lead is more formidable. It is possible that extrapolations for this metal are unjustified, but this appears to be unlikely in light of the relatively low melting point. Extrapolations here cover a range of roughly only 300°K whereas for aluminum the span is more than twice as great; for the other fcc entries extrapolations span a thousand degrees or more.

A plausible explanation may be found in the neutron-scattering work of Brockhouse *et al.*[21] An analysis of the experimental 100°K dispersion curves measured in specific crystal directions shows that in order to fit the data meaningfully one must include interactions out to at least fifth-order neighbors. Brockhouse *et al.* conclude that, "because of the long range (of the forces in lead), it is not possible to obtain a detailed description of the force constants in the Born–von Kármán theory." Until more is known about the frequency distribution for lead at elevated and room temperatures, no statement supporting or refuting the Lindemann theory can be made.

Gilvarry[2] interpreted the discrepancy between δ_f for Al and Pb as a refutation of the Lindemann law. Our results show that the more accurate lattice dynamical method gives results in only slight disagreement. More important, aluminum is consistent with most of the other fcc metals. Our results for Pb are the least reliable.

MELTING SLOPES

A test of the Lindemann law is to evaluate dT_M/dP. Equations (9) and (12) may be solved for T_M and logarithmically differentiated yielding

$$\frac{d\ln T_M}{dP}=\left.\frac{\partial \ln c}{\partial P}\right|_M+\left.\frac{1}{V}\frac{\partial V}{\partial P}\right|_M-\left.\frac{\partial \ln y}{\partial P}\right|_M, \tag{13}$$

where

$$c=c_{44},\qquad y=y_f,\quad \text{fcc from Eq. (9)},$$

$$c=c_{11}-c_{12}+4c_{44},\quad y=y_b,\quad \text{bcc from Eq. (12)},$$

and derivatives are taken along the melting curve. We use the two identities

$$\left.\frac{\partial c}{\partial P}\right|_M=\left.\frac{\partial c}{\partial P}\right|_T+\left.\frac{\partial c}{\partial T}\right|_P\frac{dT_M}{dP}, \tag{14}$$

$$\frac{1}{K_M}=-\left.\frac{1}{V}\frac{\partial V}{\partial P}\right|_M=\frac{1}{K_T}-\alpha\frac{dT_M}{dP}. \tag{15}$$

After some algebra one finds

$$\begin{aligned}\frac{dT_M}{dP}=&\left\{\left.\frac{\partial \ln c_{44}}{\partial P}\right|_T\left(1-\frac{z_f}{2y_f}\right)-\frac{1}{K_T}\left(1-\frac{z_f}{6y_f}\right)-\frac{x_f}{8c_{44}^2y_f}\right.\\&\left.\times\left[c_{44}\left(\left.\frac{\partial c_{11}}{\partial P}\right|_T-\left.\frac{\partial c_{12}}{\partial P}\right|_T\right)-(c_{11}-c_{12})\left.\frac{\partial c_{44}}{\partial P}\right|_T\right]\right\}\\&\times\left\{\frac{1}{T_M}\left(1-\frac{z_f}{y_f}\right)-\left.\frac{\partial \ln c_{44}}{\partial T}\right|_P\left(1-\frac{z_f}{2y_f}\right)+\frac{x_f}{8c_{44}^2y_f}\right.\\&\times\left[c_{44}\left(\left.\frac{\partial c_{11}}{\partial T}\right|_P-\left.\frac{\partial c_{12}}{\partial T}\right|_P\right)-(c_{11}-c_{12})\left.\frac{\partial c_{44}}{\partial T}\right|_P\right]\\&\left.-\alpha\left(1-\frac{z_f}{6y_f}\right)\right\}^{-1}\quad\text{for fcc's},\end{aligned} \tag{16}$$

$$\begin{aligned}\frac{dT_M}{dP}=&\left\{\left.\frac{\partial \ln c}{\partial P}\right|_T\left(1+\frac{4x_bc_{44}}{y_bc}-\frac{z_b}{2y_b}\right)-\frac{1}{K_T}\left(1-\frac{z_b}{6y_b}\right)\right.\\&\left.-\frac{4x_b}{y_bc}\left.\frac{\partial c_{44}}{\partial P}\right|_T\right\}\left\{\frac{1}{T_M}\left(1-\frac{z_b}{y_b}\right)+\frac{4x_b}{y_bc}\left.\frac{\partial c_{44}}{\partial T}\right|_P\right.\\&\left.\times\left(1+\frac{4x_bc_{44}}{y_bc}-\frac{z_b}{2y_b}\right)-\alpha\left(1-\frac{z_b}{6y_b}\right)\right\}^{-1}\end{aligned} \tag{17}$$

---

[19] L. Cartz, Proc. Phys. Soc. (London)**B68**, 957 (1955).

[20] G. A. Alers, J. R. Neighbours, and H. Sato, J. Phys. Chem. Solids **13**, 40 (1960).

[21] B. N. Brockhouse, T. Arase, G. Caglioti, K. R. Rao, and A. D. B. Woods, Phys. Rev. **128**, 1099 (1962).

for bcc's. Here

$$x_f = \partial y_f / \partial \gamma \,, \tag{18}$$

$$z_f = u_L \partial y_f / \partial u_L \,, \tag{19}$$

in Eq. (16), and

$$x_b = \partial y_b / \partial \gamma \,, \tag{20}$$

$$z_b = u_L \partial y_b / \partial u_L \,, \tag{21}$$

and $c = c_{11} - c_{12} + 4c_{44}$ in Eq. (17). Further we use the identity

$$1/K_T = 3/(c_{11} + 2c_{12}) + T_M V \alpha^2 / C_P \tag{22}$$

in (16) and (17), where C_P is the specific heat at constant pressure.

We have calculated the initial slopes of the melting curves of the metals Na, K, Al, Cu, Ag, and Au using the third-order elastic constants of Barsch and Chang[22] and the data of Miller and Schuele[23] for Pb. The results are presented in Table. V For purposes of comparison results of calculations are given using recent data for the pressure derivatives of the elastic constants of Cu, Ag, and Au,[24] and for the pressure and temperature derivatives of the elastic constants of Al.[25]

All of the third-order elastic constants used are those measured at room conditions, whereas Eqs. (16) and (17) require quantities evaluated at the zero-pressure melting point. Miller and Schuele have obtained measurements of the pressure derivatives of the elastic constants of lead at temperatures of 195 and 296°K, and we have extrapolated these data to the one atmosphere melting point. Results of this calculation are also presented in Table V.

TABLE V. dT_M/dP for seven cubic metals.

Element	dT_M/dP Theoretical	dT_M/dP Experimental
Sodium bcc	5.95[a]	8.0[b]
Potassium	11.68[a]	15.3[b]
Aluminum fcc	5.01[a] 3.03[d]	5.9[c]
Copper	2.98[a] 3.06[f]	3.95[e]
Silver	4.67[a] 6.09[f]	5.87[e]
Gold	4.65[a] 3.87[f]	6.12[e]
Lead	4.77[g] 5.63[i]	6.5[h]

[a] See Ref. 22.

[b] R. C. Newton, A. Jayaraman, and G. C. Kennedy, J. Geophys. Res. **67**, 2559 (1962).

[c] A. Jayaraman, W. Klement, Jr., R. C. Newton, and G. C. Kennedy, J. Phys. Chem. Solids **24**, 7 (1963).

[d] See Ref. 25.

[e] L. H. Cohen, W. Klement, Jr., and G. C. Kennedy, Phys. Rev. **145**, 519 (1966).

[f] See Ref. 24.

[g] See Ref. 23.

[h] G. C. Kennedy and R. C. Newton in *Solids Under Pressure* (McGraw-Hill Book Co., New York, 1963), p. 171.

[i] Data on pressure derivatives taken from Ref. 23 and extrapolated to melting.

The theoretical results in Table V are uniformly too low, although qualitatively of the correct magnitude. In the case of lead the use of the extrapolated pressure derivatives improves the agreement significantly. It is unfortunate that the temperature derivatives are themselves obtained by a finite difference procedure which makes a meaningful extrapolation of the temperature derivatives to melting impossible unless greater accuracy were obtainable. In view of the improvement in the calculations of the Lindemann parameter obtained by using data at the melting point, it would be valuable to use data at elevated temperatures when such data become available.

ACKNOWLEDGMENTS

The author wishes to acknowledge the guidance of his advisor Professor Leon Knopoff with this problem, especially his suggestion to include the section on melting slopes and in addition for considerable editorial advice. Also, the consistent and thoughtful encouragement of Dr. William Ofman is greatly appreciated. I thank Professor J. Trivisonno who kindly offered preprints of his work on the alkali metals. This research was supported in part by National Science Foundation Grant No. NSF GP 7764.

APPENDIX: MOMENT METHOD FOR FACE-CENTERED LATTICES

We express the frequency distribution as a series in Legendre polynomials. Since $g(x)$ is an even function, we use only the even polynomials and find

$$g(x) = \sum_{n=0}^{\infty} A_{2n} P_{2n}(x) \,, \tag{A1}$$

$$A_{2n} = (4n+1) \int_0^1 g(x) P_{2n}(x) dx \,, \tag{A2}$$

where $x = \omega/\omega_L$ with ω_L the maximum frequency and g normalized so that $\int_0^1 g(x)dx = 1$. We truncate the series at $n=6$, in which case an artificial constant term remains. The magnitude of this term in comparison with the complete function will be a qualitative indication of the accuracy of the seven term series.

We define dimensionless moments

$$\mu_{2k} = \int_0^1 x^{2k} g(x) dx \,, \quad 0 < \mu_{2k} \leq 1 \,. \tag{A3}$$

The coefficients can now be expressed in terms of these moments. The first few are

$$\begin{aligned} A_0 &= \mu_0 = 1 \,, \\ A_2 &= \tfrac{5}{2}(3\mu_2 - \mu_0) \,, \\ A_4 &= 9(35\mu_4 - 30\mu_2 + 3\mu_0)/8 \,, \end{aligned} \tag{A4}$$

---

[22] G. R. Barsch and Z. P. Chang, Phys. Status Solidi **19**, 139 (1967).

[23] R. A. Miller and D. E. Schuele, J. Phys. Chem. Solids **30**, 589 (1969).

[24] Y. Hiki and A. V. Granato, Phys. Rev. **144**, 411 (1966).

[25] J. F. Thomas, Jr., Phys. Rev. **175**, 955 (1968).

and, in general,

$$A_{2n}=(4n+1)P_{2n}(x)\,|_{x^{2k}=\mu_{2k}}\,,$$

where the $2k$th power of x ($k=0$ included) is replaced by by μ_{2k}.

The secular equation may be expressed in the form

$$\begin{aligned}&y^3+py^2+qy+r=0\,,\quad y=m\omega^2/2\alpha_1\,,\\&p=-(a_{11}+a_{22}+a_{33})\,,\\&q=a_{11}a_{22}+a_{11}a_{33}+a_{22}a_{33}-a_{23}{}^2-a_{12}{}^2-a_{13}{}^2\,,\qquad\text{(A5)}\\&r=-a_{11}a_{22}a_{33}+a_{11}a_{23}{}^2+a_{22}a_{13}{}^2+a_{33}a_{12}{}^2-2a_{12}a_{13}a_{23}\,,\end{aligned}$$

where the a_{ij} are the six independent elements of the secular determinant,[7] and each is a trigonometric function of the direction of propagation. The three roots of Eq. (A5) correspond to the three branches of the dispersion curve. Call these roots y_1, y_2, y_3, $y_i\neq 0$. All partial moments are obtained by multiplying Eq. (A5) by y^{n-3} and summing over the three values of i. Thus we have the iteration

$$\sum_{i=1}^{3} y_i{}^n=-p\sum_i y_i{}^{n-1}-q\sum_i y_i{}^{n-2}-r\sum_i y_i{}^{n-3}\qquad\text{(A6)}$$

where

$$\sum_i y_i{}^0=3\,,\quad \sum_i y_i=-p\,,\quad \sum_i y_i{}^2=-2q+p^2\,.$$

The total moments are found by summing Eq. (A6) over all directions of propagation. All sums which arise are of the form

$$\sum_{a=-N}^{N}\cos^k\frac{\pi a}{N}\quad\text{and}\quad\sum_{a=-N}^{N}\sin^k\frac{\pi a}{N}$$

and have been performed by Montroll.[4] We have used the IBM FORMAC[26] compiler for assistance in computing the higher moments. Since the roots of the secular equation are densely packed on the interval $0\leq x\leq 1$, summations are equivalent to integrals, i.e.,

$$\mu_{2n}=\frac{1}{3(2N)^3}\sum_{a=-N}^{N}\sum_{a_2=-N}^{N}\sum_{a_3=-N}^{N}\sum_{i=1}^{3}\left(\frac{\omega_i}{\omega_L}\right)^{2n}.\qquad\text{(A7)}$$

We illustrate the calculation with the simplest nontrivial case μ_2. From Eqs. (A5) and (A6)

$$\sum_i y_i=\frac{m}{2\alpha_1}\sum_i\omega_i{}^2=a_{11}+a_{22}+a_{33}\,,\qquad\text{(A8)}$$

$$\langle\omega^2\rangle=\frac{1}{3(2N)^3}\sum_{a_1,a_2,a_3}\Big(\sum_i\omega_i{}^2\Big)=\frac{2\alpha_1}{m}\frac{1}{(2N)^3}\sum_{a_1,a_2,a_3}a_{11}\,,\qquad\text{(A9)}$$

where the last result is a consequence of the symmetries involved in the triple summation. Substituting for a_{11}[7]

$$\langle\omega^2\rangle=\frac{2\alpha_1}{m}\frac{1}{(2N)^3}\sum_{a_1,a_2,a_3}(2-c_1c_2-c_1c_3+2s_1{}^2\alpha_2/\alpha_1)\,,\qquad\text{(A10)}$$

where $c_i=\cos(\pi a_i/N)$ and $s_i=\sin(\pi a_i/N)$. Carrying out the summations we find

$$\langle\omega^2\rangle=2\alpha_1(2+\alpha_2/\alpha_1)/m\qquad\text{(A11)}$$

correct to order $1/N$.

The results for all the even moments $\langle(m\omega^2/4\alpha_1)^n\rangle$, through the twelfth, are given in Table VI as a power series in α_2/α_1,

$$\langle(m\omega^2/4\alpha_1)^n\rangle=\sum_{m=0}^{n}d_{nm}(\alpha_2/2\alpha_1)^m\,.\qquad\text{(A12)}$$

Thus the nth moment of ω^2 is a power series of order n in α_2/α_1.

To calculate the dimensionless moments of Eq. (A3), one needs the maximum frequency. This is[27]

$$\omega_L{}^2=8\alpha_1/m\,.\qquad\text{(A13)}$$

Then from Eqs. (A12) and (A13)

$$\mu_{2n}=\frac{1}{2^n}\sum_{m=0}^{n}d_{nm}(\alpha_2/2\alpha_1)^m\,.\qquad\text{(A14)}$$

It is convenient to define a parameter $\gamma=1+\alpha_2/2\alpha_1$. The coefficients in the series

$$\mu_{2n}=\sum_{j=0}^{n}u_{nj}\gamma^j\qquad\text{(A15)}$$

are readily calculated from Eq. (A14) and Table VI. They are listed in Table VII.

From the moments in Eq. (A15), the expansion coefficients are found using Eq. (A4). Instead of listing

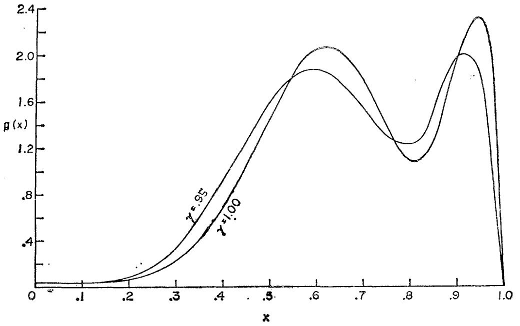

FIG. 1. Frequency spectrum for a fcc lattice approximated by $g(x)=\sum_{n=0}{}^6 a_{2n}(\gamma)P_{2n}(x)$ for two values of γ.

---

[26] *PL*/1-FORMAC Interpreter User's Reference Manual, Contributed Program Library 360*d* 03.3.004, IBM–Boston Programming Center, 545 Technology Square, Cambridge, Mass. 02139.

[27] R. Leighton, Rev. Mod. Phys. **20**, 165 (1948).

TABLE VI. Coefficients d_{nm} in $\langle (m\omega^2/4\alpha_1)^n \rangle = \sum_{m=0}^{n} d_{nm}(\alpha_2/2\alpha_1)^m$.

$n \backslash m$	0	1	2	3	4	5	6
0	1						
1	1	1					
2	5/4	2	2/3				
3	57/32	15/4	9/2	5/2			
4	703/256	115/16	179/16	10	35/8		
5	4549/1024	3585/256	3415/128	1975/64	175/8	63/8	
6	30353/4096	3513/128	63669/1024	2803/32	1287/16	189/4	231/16

TABLE VII. Coefficients u_{nj} in $\mu_{2n} = \sum_{j=0}^{n} u_{nj}\gamma^j$.

$n \backslash j$	0	1	2	3	4	5	6
0	1						
1	0	1/2					
2	3/16	$-1/4$	3/8				
3	1/256	9/32	$-3/8$	5/16			
4	287/4096	$-43/256$	119/256	$-15/32$	35/128		
5	$265/2^{15}$	$1305/2^{13}$	$-1715/2^{12}$	$1415/2^{11}$	$-35/64$	63/256	
6	$8901/2^{18}$	$-3201/2^{15}$	$26709/2^{16}$	$-1613/2^{11}$	243/256	$-315/512$	231/1024

TABLE VIII. Coefficients c_{ms} in $g(x) = \sum_{m=0}^{6} \sum_{s=0}^{6} (c_{ms}x^{2s})\gamma^m$.

	γ^0	γ^1	γ^2	γ^3	γ^4	γ^5	γ^6
x^0	+1 394.4801	−7 456.733	+16 636.377	−19 949.442	+13 684.892	−5 149.449	+839.916
x^2	−98 892.0780	+539 555.542	−1 225 395.556	+1 492 986.953	−1 039 120.729	+396 379.262	−65 513.447
x^4	+1 162 769.4146	−6 414 176.142	+14 723 600.187	−18 122 819.650	+12 738 083.381	−4 906 361.619	+818 918.090
x^6	−5 045 768.8222	+28 037 926.573	−64 830 734.783	+80 373 224.146	−56 896 499.134	+22 074 458.251	−3 712 428.675
x^8	+9 938 163.3777	−55 514 840.144	+129 050 656.239	−160 848 310.051	+114 483 821.549	−44 667 748.967	+7 557 444.089
x^{10}	−9 038 442.1118	+50 690 784.018	−118 319 751.574	+148 087 993.856	−105 852 109.181	+41 486 245.806	−7 053 614.483
x^{12}	+3 084 600.4892	−17 353 901.354	+40 638 280.270	−51 032 131.214	+36 603 290.269	−14 398 700.639	+2 458 077.774

the results of this last operation we have chosen to convert the resulting Legendre expansion to a power series in x^2. The final expression for g is

$$g(x) = \sum_{m=0}^{6} \gamma^m \sum_{s=0}^{6} c_{sm}{}^{f} x^{2s}. \tag{A16}$$

The 49 coefficients are listed in Table VIII. These coefficients are sufficient to calculate the spectrum of the face-centered lattice as an even power series of twelfth order in frequency. The spectra obtained for $\gamma = 0.95$ and 1.00 are shown in Fig. 1. The comparison of our results with those of Leighton[27] shows that the moment method describes semiquantitatively the two peaks characteristic of the fcc lattice.

We may compare the magnitude of the synthetic constant term with the average value of g in Eq. (A16). The latter is normalized to unity. In a typical case with $\gamma = 1$, the constant term has magnitude 0.04 indicating that Eq. (A16) is more accurate than might be expected.